

# Entropy and dynamic properties of water below the homogeneous nucleation temperature

Francis W. Starr<sup>1</sup>, C. Austen Angell<sup>2</sup>, Robin J. Speedy<sup>3</sup>, and H. Eugene Stanley<sup>1</sup>

<sup>1</sup>*Center for Polymer Studies, Center for Computational Science, and Department of Physics,  
Boston University, Boston, MA 02215 USA*

<sup>2</sup>*Department of Chemistry, Arizona State University, Tempe, AZ, 85287, USA*

<sup>3</sup>*7 Lindale Place, Waikanae Beach, Kapiti, New Zealand*

(July 20, 1999)

Controversy exists regarding the possible existence of a transition between the liquid and glassy states of water. Here we use experimental measurements of the entropy, specific heat, and enthalpy of both liquid and glassy water to construct thermodynamically-plausible forms of the entropy in the difficult-to-probe region between 150 K and 236 K. We assume there is no discontinuity in the entropy of the liquid in this temperature range, and use the Adam-Gibbs theory – which relates configurational entropy to dynamic behavior – to predict that dynamic quantities such as the diffusion constant and the viscosity pass through an inflection where the liquid behavior changes from that of an extremely “fragile” liquid to that of a “strong” liquid.

It has been evident for at least three decades that there is a problem connecting the thermodynamic behavior of water at normal temperatures to that of glassy water (which is found below a glass transition temperature  $T_g \approx 136$  K) [1,2]. Some contributions assert that the liquid and glassy states should be thermodynamically continuous, based on measurements of, e.g., specific heat, entropy, and relaxation times [3–7]. Other contributions argue that the liquid and glass should be thermodynamically distinct [2,8–10]. In particular, refs. [6,10] focus on a thermodynamically-plausible form for the entropy, and determine the limits on the entropy of the glass that are consistent with the possibility of continuity. The entropy of the glass was subsequently measured [7], and found to be consistent with (but does not require) thermodynamic continuity between the liquid and glass states.

As a simple illustration of the utility of thermodynamics to identify the existence of a transition or other anomalous behavior of thermodynamic properties, suppose we examine the experimental data for the enthalpy  $H$ , entropy  $S$ , and specific heat  $C_P$  of liquid water at, e.g., 10°C and of ice Ih at, e.g., −10°C. The only way to reconcile the large differences in  $H$  and  $S$  is to hypothesize a discontinuity in  $S$  or a large “spike” in  $C_P$  in this temperature range, even without knowledge that a first-order melting transition occurs. In other words using only thermodynamic data, one can place relatively stringent limits on the thermodynamic behavior near the melting transition. Inspired by this fact, we perform test for the presence of a “dramatic change” of the liquid thermodynamics below the homogeneous nucleation temperature  $T_H$  of supercooled water and above the crystallization temperature  $T_X$  of glassy water. Specifically, we use experimental data on the specific heat, entropy, and en-

thalpy in both the liquid and glassy states to construct two thermodynamically-plausible forms of the entropy in the difficult-to-probe region between  $T_X \equiv 150$  K and  $T_H \equiv 236$  K at 1 atm [11]. We then use these forms for the entropy, in conjunction with the theory of Adam and Gibbs [12], to predict behavior of the diffusion constant and the viscosity.

To determine a reasonable form for the entropy  $S = S(T, P)$ , we first focus several of the thermodynamic properties that facilitate calculation of  $S$  in the *experimentally-accessible* region and also place strict limits on the possible behavior of  $S$  in the *difficult-to-probe* region  $T_X < T < T_H$ . We define the excess enthalpy  $H_{\text{ex}} \equiv H_{\text{liquid}} - H_{\text{crystal}}$ , the excess entropy  $S_{\text{ex}} \equiv S_{\text{liquid}} - S_{\text{crystal}}$ , the difference of the liquid and crystal entropies, and the excess specific heat

$$C_P^{\text{ex}} \equiv C_P^{\text{liquid}} - C_P^{\text{crystal}} = T \left( \frac{\partial S_{\text{ex}}}{\partial T} \right)_P. \quad (1)$$

Each of these quantities is known outside the difficult-to-probe region, and in particular at the bounds  $T_X$  and  $T_H$  of the experimentally difficult-to-probe region (Table I).

•  $T > T_H$ :  $H_{\text{ex}}(T_H) = H_{\text{liquid}}(T_H) - H_{\text{crystal}}(T_H)$  has been measured from the heat of crystallization of supercooled water [16]. We can relate measured values of  $C_P^{\text{ex}}$  to  $S_{\text{ex}}$  by integrating Eq. (1),

$$S_{\text{ex}}(T) = S_{\text{ex}}(T_M) - \int_T^{T_M} \frac{C_P^{\text{ex}}}{T} dT \quad [T < T_M] \quad (2)$$

where  $S_{\text{ex}}(T_M) = \Delta S_F$ , the entropy of fusion. We numerically evaluate the integral in Eq. (2) for  $T > T_H$ , since we know  $C_P^{\text{liquid}}$  from recent bulk sample studies at temperatures from  $T_M$  down to −29°C [15], (and by emulsion

studies down to  $-37^\circ\text{C}$  [16]), and we know  $C_P^{\text{crystal}}$  for all  $T < T_M$  [17].

- $T < T_X$ :  $H_{\text{ex}}(T_X) = H_{\text{liquid}}(T_X) - H_{\text{crystal}}(T_X)$  has been measured from the heat of crystallization of glassy water [18].  $C_P^{\text{ex}}$  below  $T_X$  is known to be very small, and may be taken to be nearly  $T$ -independent for  $T \approx T_X$ .  $S_{\text{ex}}(T_X)$  is known from the vapor pressure experiments on the glass and the crystal states [7].

- $T_X < T < T_H$ : We construct two possible forms for  $S_{\text{ex}}$  for  $T_X < T < T_H$  similar to the methods of refs. [6,10], but we now include the known value of  $S_{\text{ex}}(T_X)$ .  $S_{\text{ex}}$  and  $C_P^{\text{ex}}$  fix the endpoints and the slopes of  $S_{\text{ex}}$  at  $T_X$  and  $T_H$ , while the identity

$$H_{\text{ex}}(T_H) - H_{\text{ex}}(T_X) = \int_{T_X}^{T_H} C_P^{\text{ex}} dT = 2910 \pm 30 \text{ J/mol} \quad (3)$$

constrains the area bounded by  $C_P^{\text{ex}}$  – and so also constrains the area bounded by  $S_{\text{ex}}$ , due to Eq. (1).

Using these five thermodynamic constraints [19], we construct two possible forms of  $S_{\text{ex}}$  [Fig. 1(a)] and the corresponding  $C_P^{\text{ex}}$  [Fig. 1(b)]. Curve 1 shows the case of continuity with no transition, while curve 2 shows continuity with a previously-discussed  $\lambda$ -transition [4,13]. We obtain curve 1 in an *ad-hoc* fashion that satisfies the thermodynamic constraints. We use a closed form for  $C_P^{\text{ex}}$  and  $S_{\text{ex}}$  in the  $\lambda$ -transition case, assuming mean-field behavior [8]

$$C_P^{\text{ex}}(T) = \begin{cases} a + \frac{b_+}{\sqrt{T/T_\lambda - 1}} & T > T_\lambda \\ a + \frac{b_-}{\sqrt{1 - T/T_\lambda}} & T < T_\lambda \end{cases} \quad (4a)$$

from which we obtain

$$S_{\text{ex}}(T) = \begin{cases} S_0 + a \log T + 2b_+ \tan^{-1} \sqrt{T/T_\lambda - 1} & T > T_\lambda \\ S_0 + a \log T - 2b_- \tanh^{-1} \sqrt{1 - T/T_\lambda} & T < T_\lambda \end{cases} \quad (4b)$$

In principle, the five free parameters ( $S_0$ ,  $a$ ,  $b_\pm$ , and  $T_\lambda$ ) may be determined by the five thermodynamic constraints. However, such a procedure yields an experimentally unreasonable value of  $T_\lambda = 269 \text{ K}$ . To obtain reasonable values for the parameters, we choose  $S_{\text{ex}}(200 \text{ K}) = 3.4 \text{ J/(K}\cdot\text{mol)}$ ,  $C_P^{\text{ex}}(200 \text{ K}) = 15 \text{ J/(K}\cdot\text{mol)}$ , and  $T_\lambda = 225 \text{ K}$ . This fixes the remaining free parameters in Eq. (4) [20].

Curves 1 and 2 for  $S_{\text{ex}}$  and  $C_P^{\text{ex}}$  both show sharp changes in their behavior just below 230 K. Note that a significantly less sharp change in  $S_{\text{ex}}$  than shown would not satisfy the constraint of Eq. (3), as can also be seen by rewriting constraint (3) in terms of the area bounded by  $S_{\text{ex}}$ . From integration by-parts, we find

$$\int_{T_X}^{T_H} S_{\text{ex}} dT = [T S_{\text{ex}} - H_{\text{ex}}]_{T_X}^{T_H} = 422 \pm 30 \text{ J/mol.} \quad (5)$$

A more gradual change in  $S_{\text{ex}}$  below  $T_H$  than shown in Fig. 1(a) would bound an area  $\int_{T_X}^{T_H} S_{\text{ex}} dT$  larger than 422 J/mol. Furthermore, the inflection in  $S_{\text{ex}}$  [Fig. 1] must occur at  $T \gtrsim 215 \text{ K}$ , as moving the inflection to a significantly lower temperature would also yield an area too large.

We do not hypothesize a discontinuous form for the entropy because the magnitude of the possible discontinuity is unknown. While the data in Table I and the thermodynamic constraints do not require a discontinuity in  $S_{\text{conf}}$  below  $T_H$ , the data can not rule out the possibility. Furthermore, behavior of  $C_P^{\text{ex}}$  resembling a step-function is also possible. However, the accelerating increase of  $C_P^{\text{ex}}$  approaching the inaccessible region from above makes the  $\lambda$ -transition a more natural choice. On the other hand, we emphasize that using the available data, it is impossible to distinguish the correct form of  $C_P^{\text{ex}}$ , or the exact location of any possible transition (only that an anomaly occurs within the approximate range of  $200 \text{ K} < T < 230 \text{ K}$ ).

We now consider the possible implications of the approximate forms for  $S_{\text{ex}}$  on the dynamic behavior below  $T_H$ . The entropy-based Adam-Gibbs theory [12] has been used to describe the relaxation of liquids approaching their glass transitions [21], and provides an explanation for the variation of diffusion constant  $D$  and viscosity  $\eta$  (or other characteristic dynamic quantity) in the anomalous range below  $-20^\circ\text{C}$  [22]. We use the prediction

$$\eta = \eta_0 \exp\left(\frac{A}{T S_{\text{conf}}}\right). \quad (6)$$

Here  $A$  is a constant [23]. The configurational entropy of the liquid,  $S_{\text{conf}} \equiv S_{\text{liquid}} - S_{\text{vib}}$ , can be understood as the entropy attributable to the various basins the liquid can sample in the energy landscape picture [1,24]. The vibrational component  $S_{\text{vib}}$  of the entropy is attributable to the thermal excitation the liquid experiences in the basin sampled, so we may approximate  $S_{\text{vib}}^{\text{liquid}} \approx S_{\text{vib}}^{\text{crystal}}$ . For typical crystals,  $S_{\text{conf}} \approx 0$ , since the crystal samples a negligible number of basins. Hence  $S_{\text{crystal}} \approx S_{\text{vib}}$ , from which it follows that for the liquid  $S_{\text{conf}} \approx S_{\text{ex}}$ . The approximation  $S_{\text{vib}}^{\text{liquid}} \approx S_{\text{vib}}^{\text{crystal}}$  is quite good for liquids near  $T_g$  [25], as the liquid typically samples only the deepest basins in the energy landscape, with small harmonic excitations about the minimum, similar to the crystal behavior. At higher  $T$ , the liquid explores a much greater region of the landscape, and is no longer localized in a single basin for an extended time. Thus at higher  $T$ , the approximation that  $S_{\text{vib}}^{\text{liquid}} \approx S_{\text{vib}}^{\text{crystal}}$  may not work as well [26].

In the case of ice, there exists a residual entropy  $S_{\text{res}}$  at zero temperature due to proton disorder [29]. When we subtract  $S_{\text{crystal}}$  from  $S_{\text{liquid}}$ , we also implicitly subtract

the contribution arising from  $S_{\text{res}}$ , which should also contribute to the available configurations of the liquid, so we include  $S_{\text{res}}$  explicitly

$$S_{\text{conf}} = S_{\text{ex}} + S_{\text{res}}. \quad (7)$$

We use this form of  $S_{\text{conf}}$  to predict the behavior of  $\eta$  and  $D$  [30] for  $T \leq T_H$ . We select parameters [31] in Eq. (6) to fit the experimental values of  $D$  [32] and  $\eta$  [33] [Fig. 2]. The non-Arrhenius behavior for  $T \gtrsim 230$  K is typical for a fragile liquid [24]. As  $T \rightarrow T_g$ , we find  $\eta(T_g) \approx 10^{16}$  Poise. This is roughly 3 orders of magnitude larger than  $\eta(T_g)$  expected from experiments [35], but is not unreasonable considering that a number of approximations that were necessary, and further that we have extrapolated over 14 orders of magnitude from experimental data covering only one order of magnitude. Furthermore, excluding  $S_{\text{res}}$  in Eq. (7), results in an absurd value  $\eta(T_g) \approx 10^{43}$  Poise, emphasizing the importance of including  $S_{\text{res}}$  as part of  $S_{\text{conf}}$  [36,37].

The dramatic change in entropy around 225 K required by the physical constraints is reflected by the “kinks” that appear in  $D$  and  $\eta$  at  $T \approx 225$  K. In contrast to the fragile behavior for  $T \gtrsim 220$  K, the behavior for  $T \lesssim 220$  is characteristic of a strong liquid [24] – i.e. Arrhenius behavior with an appropriate activation energy. We find  $E_D/RT_g \approx 28$ ,  $E_\eta/RT_g \approx 29$ , larger than the expected activation energy  $E/RT_g \approx 14$  for an “ideal” strong liquid [24], but much less than that of a fragile liquid ( $E/RT_g \approx 80 - 100$ ). Furthermore, adjustment of the constants in Eq. (6) such that  $\eta(T_g) = 10^{13}$  Poise, as expected from experiments [35], yields a value of  $E_\eta/RT_g$  much closer to the “ideal” value for a strong liquid. These results support the hypothesis that the fragile behavior of water shows a change to strong behavior for  $T \lesssim 220$  K. Water is also expected to be a strong liquid near  $T_g \approx 136$  K, based on measurements of the change in  $C_P$  near  $T_g$ , and the width of the glass transition [38]. Such a crossover from fragile to strong behavior is not typical of liquids, and merits further experimental scrutiny [39].

We wish to thank B.D. Kay, S. Sastry, F. Sciortino, R.S. Smith, and M. Yamada for enlightening discussions. We especially thank C.T. Moynihan for his important contributions. FWS is supported by a NSF graduate fellowship. CAA acknowledges support from a NSF Solid State Chemistry grant DMR-9108028-002. RJS acknowledges support from the Marsden Fund through contract GRN 501. The Center for Polymer Studies is supported by NSF grant CH9728854.

- [1] P.G. Debenedetti, *Metastable Liquids* (Princeton Univ. Press, Princeton, 1996)
- [2] C.A. Angell and E.J. Sare, *J. Chem. Phys.* **52**, 1058 (1970).
- [3] C.G. Venkatesh, S.A. Rice, and A.H. Narten, *Science* **186**, 927 (1975); S.A. Rice, M.S. Bergren, and L. Swingle, *Chem. Phys. Lett.* **59**, 14 (1978); C.A. Angell and J.C. Tucker, *J. Phys. Chem.* **84**, 268 (1980); G.P. Johari, *J. Chem. Phys.* **105**, 7079 (1996).
- [4] C.A. Angell, J. Shuppert and J.C. Tucker, *J. Phys. Chem.* **77**, 3092 (1973).
- [5] G.P. Johari, A. Hallbrucker, and E. Mayer, *Nature* **330**, 552 (1987); A. Hallbrucker, E. Mayer, and G.P. Johari, *J. Phys. Chem.* **93**, 4986 (1989).
- [6] G.P. Johari, G. Fleissner, A. Hallbrucker, and E. Mayer, *J. Phys. Chem.* **98**, 4719 (1994).
- [7] R.J. Speedy, P.G. Debenedetti, R.S. Smith, C. Huang, and B.D. Kay, *J. Chem. Phys.* **105**, 240 (1996).
- [8] R. J. Speedy and C. A. Angell, *J. Chem. Phys.* **65**, 851 (1976); R. J. Speedy, *J. Chem. Phys.* **86**, 892 (1982).
- [9] G.P. Johari, *Phil. Mag.* **35** 1077 (1977); M. Sugasaki, H. Suga, and S. Seki, *Bull. Chem. Soc. Jpn.* **41**, 2591 (1968).
- [10] R.J. Speedy, *J. Phys. Chem.* **96**, 2232 (1992).
- [11] The region  $T_X < T < T_H$  is only “inaccessible” by ordinary time scale experiments. However, recent experiments have probed the liquid even at ordinary time scales by exploiting the equality of the Gibbs potential of the liquid and crystal along the metastable melting lines (see O. Mishima and H.E. Stanley, *Nature* **392**, 192 (1998)).
- [12] G. Adam and J.H. Gibbs, *J. Chem. Phys.* **43**, 139 (1965).
- [13] R.J. Speedy, *J. Phys. Chem.* **91**, 3354 (1987).
- [14] Y.P. Handa and D.D. Klug, *J. Phys. Chem.* **92**, 3323 (1988).
- [15] E. Tombari, C. Ferrari, and G. Salvetti, *Chem. Phys. Lett.* **300**, 749 (1999).
- [16] C.A. Angell, M. Oguni, and W.J. Sichina, *J. Phys. Chem.* **86**, 998 (1982).
- [17] W.F. Giaque and J.W. Stout, *J. Am. Chem. Soc.* **58**, 1144 (1936).
- [18]  $H_{\text{ex}}$  is measured by the heat released when freezing to the crystalline state. At 150 K, water freezes not to ice Ih, but to ice Ic with  $H_{\text{ex}} = 1330$  J/mol. To account for the enthalpy difference between ice Ic and Ih, we also include 50 J/mol, the heat evolved when ice Ic transforms to ice Ih. See P.Y. Harta, D.D. Klug, and E. Whalley, *J. Chem. Phys.* **84**, 7009 (1976) and A. Hallbrucker and E. Mayer, *J. Phys. Chem.* **91**, 503 (1987).
- [19] The five constraints are the known values of  $S_{\text{ex}}$  and  $C_P^{\text{ex}}$  at  $T_X$  and  $T_H$ , plus the limitation on the area bounded by  $S_{\text{ex}}$  between  $T_X$  and  $T_H$ .
- [20] The values we obtain for the  $\lambda$ -transition are:  $T_\lambda = 225$  K,  $S_0 = 34.3$  J/(K·mol),  $a = -4.8$  J/mol,  $b_+ = 16.4$  J/mol, and  $b_- = 6.6$  J/mol. We allow for the possibility that  $b_+$  and  $b_-$  differ because the prefactor on the diverging term of Eq. (4a) typically depends on whether the transition is approached from temperatures above or below  $T_\lambda$ .
- [21] J.H. McGill, *J. Chem. Phys.*, **47**, 2802 (1967); G.W. Scherer, *J. Amer. Ceram. Soc.* **67**, 504 (1984); C.A. Angell, *J. Res. NIST* **102**, 171 (1997).
- [22] C.A. Angell, E.D. Finch, L.A. Woolf and P. Bach, *J.*

Chem. Phys. **65**, 3063 (1976).

- [23] The Vogel-Fulcher-Tamman form  $\eta = \eta_0 \exp(B/(T-T_0))$  for the temperature dependence of viscosity and characteristic times of liquids at low temperature can be obtained from Eq. (6) by assuming that  $C_P^{\text{ex}} \propto T^{-1}$ . Note that  $T_0 < T_g$  is typically associated with an underlying “ideal” glass transition.
- [24] C. A. Angell, Science **267**, 1924 (1995); F. H. Stillinger, *Ibid.*, 1935 (1995).
- [25] M. Goldstein, J. Chem. Phys. **51**, 3728 (1969).
- [26] Specifically, simulations indicate that localization of the system in a single basin occurs at  $T \approx T_{\text{MCT}}$  (F. Sciortino and P. Tartaglia, Phys. Rev. Lett **78**, 2385 (1998)), where  $T_{\text{MCT}}$  is the crossover temperature of the mode-coupling theory [27]. It has been argued that  $T_{\text{MCT}} = 228$  K at 1 atm for water [28]. Hence all available data are for  $T > T_{\text{MCT}}$ . Recent simulations have shown that the approximation of separating vibrational and configurational contributions to the free energy is still valid for  $T$  somewhat larger than  $T_{\text{MCT}}$ .
- [27] W. Götze and L. Sjögren, Rep. Prog. Phys. **55**, 241 (1992).
- [28] A.P. Sokolov, J. Hurst, and D. Quitmann, Phys. Rev. B **51**, 12865 (1995); P. Gallo, *et al.*, Phys. Rev. Lett. **76**, 2730 (1996); F. Sciortino, *et al.*, Phys. Rev. E **54**, 6331 (1996); F.W. Starr *et al.*, Phys. Rev. Lett. (accepted).
- [29] The residual entropy due to proton disorder can be estimated by  $R \ln(3/2) = 3.4$  J/(K·mol) (L. Pauling, J. Am. Chem. Soc. **57**, 2680 (1935)).
- [30] We make predictions for both  $\eta$  and  $D$ . However, the decoupling of the  $D$  from  $\eta$  – evidenced by the breakdown of the Stokes-Einstein relationship at low  $T$  – leads us to believe that our predictions for  $D$  may not be accurate. The decoupling might be associated with a “normal” component of  $D$  that is not strongly affected by the dramatic increases in  $\eta$ , such as sometimes observed near critical point (J.C. Allegra, A. Stein, and G.F. Allen, J. Chem. Phys. **55**, 1716 (1971)).
- [31] For the diffusion, we use  $D_0 = 5.55 \times 10^{-4}$  cm<sup>2</sup>/s and  $A = -27.4$  kJ/mol. For the viscosity, we use  $\eta_0 = 1.99 \times 10^{-4}$  Poise and  $e = 30.4$  kJ/mol. These parameters were obtained by fitting  $S_{\text{conf}}$  to the experimental data in the region between  $T = 235$  K and 273 K.
- [32] K.T. Gillen, D.C. Douglass, and M.J.R. Hoch, J. Chem. Phys. **57**, 5117 (1972). The values of  $D$  reported are  $\approx 7\%$  too small. Increasing the measured  $D$  values by 7% would not change any conclusions presented here, and would also be indistinguishable on the scale of Fig. 1(a).
- [33] J. Hallett, Proc. Phys. Soc. **82**, 1046 (1963); Yu.A. Osipov, B.V. Zheleznyi, and N.F. Bondarenko, Zh. Fiz. Khim. **51**, 1264 (1977).
- [34] R.S. Smith and B.D. Kay, Nature **398**, 788 (1999).
- [35] G.P. Johari, J. Phys. Chem. B **102**, 4711 (1998).
- [36] C.T. Moynihan, private communication.
- [37] An alternative procedure is to fix  $\eta(T_g) \approx 10^{13}$  Poise, and determine the value of  $S$  is consistent with this  $\eta$ .
- [38] C.A. Angell, J. Phys. Chem. **97**, 6339 (1993); K. Ito, C.T. Moynihan, and C.A. Angell, Nature **398**, 492 (1999).
- [39] The expectation that water is strong near  $T_g$  does not agree with recent data [34], perhaps indicating that the Adam-Gibbs predictions are not valid for water.

TABLE I. Thermodynamic properties of water at 1 atm at 150 K and 236 K. Here,  $X_{\text{ex}} \equiv X_{\text{liquid}} - X_{\text{crystal}}$ , the excess quantity  $X$  of the liquid value relative to the ice Ih value. The uncertainties of  $S_{\text{ex}}$  and  $H_{\text{ex}}$  are taken from [13], which contains arguments supporting the reliability of the data.

	$T_X = 150$ K	$T_H = 236$ K
$C_P^{\text{ex}}$ [J/(K·mol)]	$\approx 2$ [5,6,14]	$69.2 \pm 0.5$ [15–17]
$S_{\text{ex}}$ [J/(K·mol)]	$1.7 \pm 1.7$ [7]	$15.2 \pm 0.1$ [13,16,17]
$H_{\text{ex}}$ [J/mol]	$1380 \pm 20$ [18]	$4290 \pm 20$ [13,16]

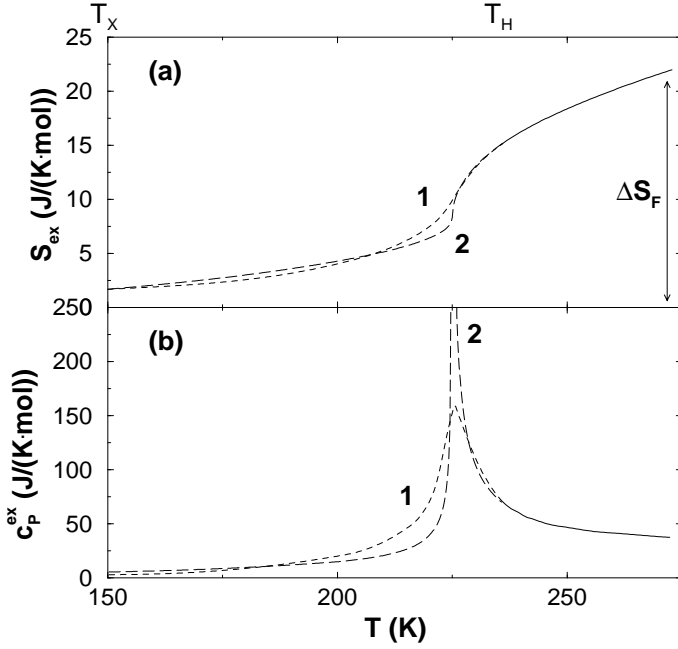


FIG. 1. (a) Possible forms for the excess entropy  $S_{\text{ex}}$  in the experimentally inaccessible region. Curve 1 corresponds to no transition, while curve 2 shows a  $\lambda$ -transition at 225 K. Any thermodynamically plausible form of  $S_{\text{ex}}$  (without a discontinuity) can vary only slightly from these form (due to the uncertainty in  $H_{\text{ex}}$ ). The entropy of fusion  $\Delta S_F = 21.8 \text{ J}/(\text{K}\cdot\text{mol})$  for freezing at 273 K is indicated by the arrow. (b) Constant pressure excess specific heat  $C_P^{\text{ex}} = T(dS_{\text{ex}}/dT)_P$  for the possible forms of  $S_{\text{ex}}$  shown in (a). Curve 2 has a diverging  $C_P^{\text{ex}}$  at the  $\lambda$ -transition temperature.

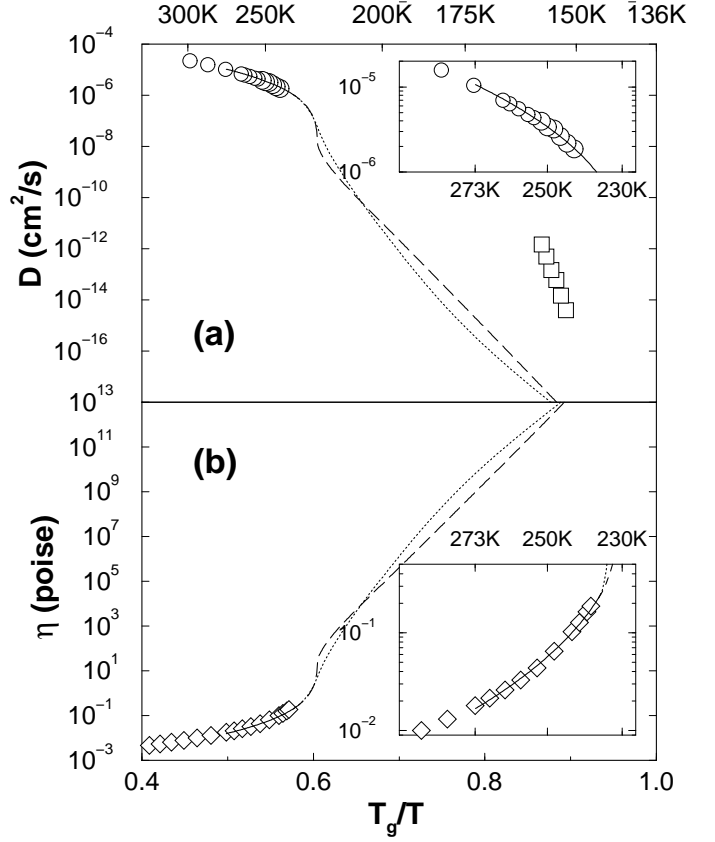


FIG. 2. (a) Diffusivity predicted by Eq. (6). The experimental data ( $\circ$ ) for  $T > 235$  K are from [32]. The data for  $T < 160$  K ( $\square$ ) are from [34]. (b) Fit of  $S_{\text{ex}}$  to viscosity using the same procedure. Experimental data ( $\diamond$ ) are from [33]. Both (a) and (b) show behavior expected for a strong liquid for  $T \lesssim 220$  K – i.e. Arrhenius behavior with an activation energy  $\approx T_g/3$  (in units of  $\text{kJ}/\text{mol}$ ) [24]. The insets show the quality of the fit in the region where experimental data are available.